

Non-Gaussian statistics and optical rogue waves in stimulated Raman scattering

YASHAR E. MONFARED AND SERGEY A. PONOMARENKO*

Department of Electrical and Computer Engineering, Dalhousie University, Halifax, NS, B3J 2X4 Canada
*serpo@dal.ca

Abstract: We explore theoretically and numerically optical rogue wave formation in stimulated Raman scattering inside a hydrogen filled hollow core photonic crystal fiber. We assume a weak noisy Stokes pulse input and explicitly construct the input Stokes pulse ensemble using the coherent mode representation of optical coherence theory, thereby providing a link between optical coherence and rogue wave theories. We show that the Stokes pulse peak power probability distribution function (PDF) acquires a long tail in the limit of nearly incoherent input Stokes pulses. We demonstrate a clear link between the PDF tail magnitude and the source coherence time. Thus, the latter can serve as a convenient parameter to control the former. We explain our findings qualitatively using the concepts of statistical granularity and global degree of coherence.

© 2017 Optical Society of America

OCIS codes: (030.0030) Coherence and statistical optics; (030.6600) Statistical optics; (190.4370) Nonlinear optics, fibers.

References and links

1. J. M. Dudley, F. Dias, M. Erkintalo and G. Genty, "Instabilities, breathers, and rogue waves in optics," *Nature Photon.* **8**, 755–764 (2014).
2. D. R. Solli, C. Ropers, P. Koonath and B. Jalali, "Optical rogue waves," *Nature (London)* **450**, 1054–1057 (2007).
3. N. Akhmediev, B. Kibler, F. Baronio, M. Belic, W-P Zhong, Y. Zhang, W. Chang, J. M. Soto-Crespo, P. Vouzas, P. Grelu, C. Lecaplain, K. Hammani, S. Rica, A. Picozzi, M. Tlidi, K. Panajotov, A. Mussot, A. Bendahmane, P. Szriftgiser, G. Genty, J. Dudley, A. Kudlinski, A. Demircan, U. Morgner, S. Amiranashvili, C. Bree, G. Steinmeyer, C. Masoller, N. G. R. Broderick, A. F. J. Runge, M. Erkintalo, S. Residori, U. Bertolozzo, F. T. Arecchi, S. Wabnitz, C. G. Tiofack, S. Coulibaly and M. Taki, "Roadmap on optical rogue waves and extreme events," *J. Opt.* **18**, 063001 (2016).
4. M. Onorato, S. Residori, U. Bertolozzo, A. Montina and F. T. Arecchi, "Rogue waves and their generating mechanisms in different physical contexts," *Phys. Rep.* **528**, 47–89 (2013).
5. N. Akhmediev, J. M. Dudley, D. R. Solli, and S. K. Turitsyn, "Recent progress in investigating optical rogue waves," *J. Opt.* **15**, 060201 (2013).
6. A. Montina, U. Bertolozzo, S. Residori, and F. T. Arecchi, "Non-Gaussian statistics and extreme waves in a nonlinear optical cavity," *Phys. Rev. Lett.* **103**, 173901 (2009).
7. S. Residori, U. Bertolozzo, A. Montina, F. Lenzini and F. T. Arecchi, "Rogue waves in spatially extended optical systems," *Fluctuat. Noise Lett.* **11**, 1240014 (2009).
8. J. M. Soto-Crespo, Ph. Grelu and N. Akhmediev, "Dissipative rogue waves: extreme pulses generated by passively mode-locked lasers," *Phys. Rev. E* **84**, 016604 (2011).
9. A. Zavyalov, O. Egorov, R. Iliev and F. Lederer, "Rogue waves in mode-locked fiber lasers," *Phys. Rev. A* **85**, 013828 (2012).
10. A. F. J. Runge, N. G. R. Broderick, and M. Erkintalo, "Observation of soliton explosions in a passively mode-locked fiber laser," *Optica* **2**, 36-39 (2015).
11. J. He, S. Xu and K. Porsezian, "New types of rogue wave in an erbium-doped fiber system," *J. Phys. Soc. Japan* **81**, 033002 (2012).
12. K. Hammani, C. Finot, J. M. Dudley and G. Millot, "Optical rogue-wave-like extreme value fluctuations in fiber Raman amplifiers," *Opt. Express* **16**, 16467–16473 (2008).
13. J. Kasparian, P. Béjot, J.-P. Wolf, and J. M. Dudley, "Optical rogue wave statistics in laser filamentation," *Opt. Express* **17**, 12070–12075 (2009).
14. D. Majus, V. Jukhna, G. Valiulis, D. Facciao and A. Dubietis, "Spatiotemporal rogue events in femtosecond filamentation," *Phys. Rev A* **83**, 025802 (2011).
15. K. Hammani, C. Finot and G. Millot, "Emergence of extreme events in fiber-based parametric processes driven by a partially incoherent pump wave," *Opt. Lett.* **34**, 1138–1140 (2009).
16. F. T. Arecchi, U. Bertolozzo, A. Montina and S. Residori, "Granularity and inhomogeneity are joint generators of optical rogue waves," *Phys. Rev. Lett.* **106**, 153901 (2011).

17. R. Höhmann, U. Kuhl, H-J. Stöckmann, L. Kaplan and E. J. Heller, "Freak waves in the linear regime: a microwave study," *Phys. Rev. Lett.* **104**, 093901 (2010).
18. D. H. Peregrine, "Water waves nonlinear Schrödinger equations and their solutions," *J. Aust. Math. Soc. Ser. B* **25**, 16–43 (1983).
19. N. Akhmediev, A. Ankiewicz, and M. Taki, "Waves that appear from nowhere and disappear without a trace," *Phys. Lett. A*, **373**, 675–678 (2009).
20. V. I. Shrira and V. V. Geogjaev, "What makes Peregrine soliton so special as a prototype of freak waves?" *J. Eng. Math.* **67**, 11–12 (2010).
21. N. Akhmediev, J. M. Soto-Crespo, and A. Ankiewicz, "How to excite a rogue wave," *Phys. Rev. A* **80**, 043818 (2009).
22. S. Toenger, T. Godin, C. Billet, F. Dias, M. Erkintalo, G. Genty, and J. M. Dudley, "Emergent rogue wave structures and statistics in spontaneous modulation instability," *Sci. Rep.* **5**, 10380 (2015).
23. B. Kibler, A. Chabchoub, A. Gelash, N. Akhmediev, and V. E. Zakharov, "Superregular Breathers in Optics and Hydrodynamics: Omnipresent Modulation Instability beyond Simple Periodicity," *Phys. Rev. X*, **5**, 041026 (2015).
24. B. Kibler, J. Fatome, C. Finot, G. Millot, F. Dias, G. Genty, N. Akhmediev, and J. M. Dudley, "The Peregrine soliton in nonlinear fiber optics," *Nat. Phys.* **6**, 790–795 (2010).
25. B. Kibler, J. Fatome, C. Finot, G. Millot, G. Genty, B. Wetzel, N. Akhmediev, F. Dias, and J. M. Dudley, "Observation of Kuznetsov-Ma soliton dynamics in optical fiber," *Sci. Rep.* **2**, 463 (2012).
26. A. Picozzi, J. Garnier, T. Hanson, P. Suret, S. Randoux, G. Millot, and D. N. Christodoulides, "Optical wave turbulence: toward a unified thermodynamic formulation of statistical nonlinear optics," *Phys. Rep.* **542**, 1–132 (2014).
27. P. Walczak, S. Randoux, and P. Surret, "Optical Rogue Waves in Integrable Turbulence," *Phys. Rev. Lett.* **114**, 143903 (2015).
28. P. Surret, R. El Koussaifi, A. Tikan, C. Evain, S. Randoux, C. Szwaj, and S. Bielawski, "Single-shot observation of optical rogue waves in integrable turbulence using microscopy," *Nat. Commun.* **7**, 13136 (2016).
29. J. M. Soto-Crespo, N. Devine, and N. Akhmediev, "Integrable Turbulence and Rogue Waves: Breathers or Solitons?" *Phys. Rev. Lett.* **116**, 103901 (2016).
30. N. Akhmediev, J. M. Soto-Crespo, and N. Devine, "Rogue waves, probability density functions and spectral features," *Phys. Rev. E* **94**, 022212 (2016).
31. D. Agafontsev and V. E. Zakharov, "Integrable turbulence and formation of rogue waves," *Nonlinearity* **28**, 2791 (2015).
32. V. E. Zakharov, "Turbulence in integrable systems," *Stud. Appl. Math.* **122**, 219–234 (2010).
33. M. Taki, A. Mussot, A. Kudlinski, E. Louvergneaux, M. Kolobov, and M. Douay, "Third-order dispersion for generating optical solitons," *Phys. Rev. A* **374**, 691–695 (2010).
34. K. Hammani, B. Kibler, C. Finot, and A. Picozzi, "Emergence of rogue waves from optical turbulence," *Phys. Lett. A* **374**, 3585–3589 (2010).
35. B. Kibler, K. Hammani, C. Michel, C. Finot, and A. Picozzi, "Rogue waves, rational solitons and wave turbulence theory," *Phys. Lett. A* **375**, 3149–3155 (2011).
36. L. Allen and J. H. Eberly, *Optical resonance and two-level atoms*, (Dover Publications Inc., New York, 1975).
37. L. Mokhtarpour and S. A. Ponomarenko, "Fluctuating pulse propagation in resonant nonlinear media: self-induced transparency random phase soliton formation," *Opt. Express* **23**, 30270–30282 (2015).
38. A. Betlej, P. Schmitt, P. Sidereas, R. Tracy, C. G. Goedde, and J. R. Thompson, "Increased Stokes pulse energy variation from amplified classical noise in a fiber Raman generator," *Opt. Express* **13**, 2948–2960 (2005).
39. E. Landahl, D. Baiocchi, and J. R. Thompson, "A simple analytical model for noise shaping by an optical fiber generator," *Opt. Commun.* **150**, 339–347 (1998).
40. A. S. Grabtchikov, A. I. Vodtchits, and V. A. Orlovich, "Pulse-energy statistics in the linear regime of stimulated Raman scattering with a broad-band pump," *Phys. Rev. A*, **56**, 1666–1669 (1997).
41. F. Benabid, G. Bouwmans, J. C. Knight, and P. St. J. Russell, "Ultra-high Efficiency Laser Wavelength Conversion in a Gas-Filled Hollow Core Photonic Crystal Fiber by Pure Stimulated Rotational Raman Scattering in Molecular Hydrogen," *Phys. Rev. Lett.* **93**, 123903 (2004).
42. A. Nazarkin, A. Abdolvand, A. V. Chugreev, and P. St. J. Russell, "Direct Observation of Self-Similarity in Evolution of Transient Stimulated Raman Scattering in Gas-Filled Photonic Crystal Fibers," *Phys. Rev. Lett.* **105**, 173902 (2010).
43. F. Belli, A. Abdolvand, W. Chang, J. C. Travers, and P. St. J. Russell, "Vacuum-ultraviolet to infrared supercontinuum in hydrogen-filled photonic crystal fiber," *Optica* **2**, 292–300 (2015).
44. F. Flora and L. Giudicotti, "Complete calibration of a Thomson scattering spectrometer system by rotational Raman scattering in H₂," *Appl. Opt.* **26**, 4001–4008 (1987).
45. L. Mandel and E. Wolf, *Optical Coherence and Quantum Optics* (Cambridge University Press, 1995).
46. A. Papoulis, *Probability Random Variables, and Stochastic Processes* (McGraw Hill, 1991) 3rd Ed.
47. J. W. Goodman, *Statistical Optics* (Wiley, 1985).
48. M. Qasymeh, M. Cada and S. A. Ponomarenko, "Quadratic Electro-Optical Kerr Effect: Application to Photonic Devices," *IEEE J. Quant. Electron.* **44**, 740–746 (2008).
49. F. Y., F. Chu and A. C. Scott, "Inverse scattering transform for wave-wave scattering," *Phys. Rev. A* **12**, 2060–2064

(1975).

50. C. R. Menyuk, "Transient solitons in stimulated Raman scattering," *Phys. Rev. Lett.* **62**, 2937–2940 (1989).

1. Introduction

Optical rogue waves (ORWs) are rare and uncommonly large amplitude statistical optical waves with heavy-tailed probability distributions [1]. The pioneering work of Solli *et al* on ORW excitation in supercontinuum generation in optical fibers [2] has triggered a tsunami of publications on ORWs in various contexts [3–5]. The vast majority of ORW research has so far focused on the modulation instability excitation scenario within the framework of integrable nonlinear Schrödinger equation [4]. Yet, optical rogue waves have also been theoretically predicted and/or experimentally demonstrated in such diverse systems as optical cavities [6, 7], passively mode-locked fiber lasers [8–10], erbium-doped fiber systems [11], Raman fiber amplifiers [12], spatiotemporal structures and laser filamentation [13, 14], parametric processes [15] and even in linear light propagation inside multimode fibers [16] as well as in microwave settings [17]. To date, several coherent structures such as the Peregrine soliton [1, 18–20], solitons on finite background [1, 19, 21, 22], and superregular breathers [23] have been conjectured to serve as ORW prototypes in weakly dispersive, weakly nonlinear wave systems described by the integrable 1D nonlinear Schrödinger equation. These predictions have prompted elegant experiments aiming to realize such coherent ORW prototypes in highly controlled environments in fiber optics [24, 25].

On the other hand, the role played by source coherence in shaping emergent nonlinear wave structures is a fundamental issue in nonlinear statistical optics [26]. In this context, the ORW generation with random sources has lately triggered growing interest. In particular, the source coherence influence on the ORW emergence has been examined both numerically [27–31] and experimentally [27, 28] and a pronounced sensitivity of the peak wave power probability density function (PDF) shape to random initial conditions was established. The above results were obtained for 1D wave turbulence described by the nonlinear Schrödinger equation within the framework of integrable turbulence [32]. The ORW excitation in nearly integrable, Hamiltonian nonlinear systems with noisy input waves was also studied [33–35].

To our knowledge however, the work on ORW excitation with random sources has so far been limited to optical waves far away from internal medium resonances. Yet, resonant light-matter interactions are known to strongly enhance media nonlinearity, dispersion and absorption, giving rise to a host of new nonlinear phenomena such as electromagnetically- and self-induced transparency [36]. Lately, self-induced transparency and the ensuing random phase soliton formation with statistical light has been explored in resonant nonlinear media in the two-level approximation [37]. Thus, the ORW emergence in resonant nonlinear media is of fundamental interest. In this context, we anticipate stimulated Raman scattering (SRS) in optical fibers to be a fertile ground for ORW exploration. The latter arise naturally in SRS as either noise is irreversibly transferred from the pump to amplified Stokes waves or the noise present in a seeded Stokes wave is amplified as the Stokes amplitude is amplified, leading to a heavy-tailed probability distribution of the Stokes wave peak power. The first mechanism was explored in SRS generation in highly nonlinear solid-core fibers in the picosecond pulse regime [12]. Although the influence of pump noise on the Stokes pulse characteristics in SRS generation from quantum noise in the nanosecond regime was examined in detail [38–40], no explicit connection to rogue waves was made. Moreover, the ORW excitation in the SRS amplification regime with a noisy Stokes input present has not, to our knowledge, been addressed. A related fundamental issue concerns rogue wave control in the nanosecond SRS regime. The issue has also a practical dimension in light of recent efforts to realize novel SRS and supercontinuum generation regimes, controllable over long interaction lengths inside hollow core photonic crystal fibers [41–43].

In this work, we numerically study SRS in the amplification regime of a weak noisy probe Stokes pulse, mediated by a strong coherent Raman pump pulse inside a hydrogen filled hollow

core photonic crystal fiber (HC PCF). We show that nonlinear noise amplification, concurrent with the Stokes pulse amplitude growth, skews the Stokes pulse peak power statistics, converting it to a heavy-tailed non-Gaussian one which is a statistical signature of rogue wave excitation. We model fluctuating input Stokes pulses as a Gaussian random process. We explicitly construct the input Stokes pulse ensemble using the coherent mode representation of optical coherence theory. Our approach has two major benefits. First, we establish a link between fundamental concepts of optical coherence theory such as coherence time and global degree of coherence of the source and the generated rogue wave statistics. Second, we show that the source coherence time can serve as a versatile control parameter for ORW excitation in the system. In particular, we show how the Stokes power distribution tail can be enlarged or shortened by simply adjusting the Stokes input coherence time. We explain our findings qualitatively using the concepts of statistical granularity and global degree of coherence.

2. Theoretical formulation and statistical source description

We start by considering the standard SRS equations, written in a moving reference frame, $\tau = t - \beta_1 z$, where β_1 is an inverse group velocity assumed to be the same for co-propagating pump and Stokes pulses. The wave equations for the slowly-varying pump E_p and Stokes E_s amplitudes read

$$\partial_\zeta E_p = \left(\frac{i\omega_p N r_{eff}}{2\epsilon_0 c n_p} \right) \sigma E_s \quad (1)$$

and

$$\partial_\zeta E_s = \left(\frac{i\omega_s N r_{eff}}{2\epsilon_0 c n_s} \right) \sigma^* E_p, \quad (2)$$

and the Schrödinger equation for the medium dipole matrix element σ can be written in the weak excitation limit as

$$\partial_\tau \sigma = -\gamma \sigma + \left(\frac{i r_{eff}}{4\hbar} \right) E_s^* E_p. \quad (3)$$

Here $\omega_{p,s}$ and $n_{p,s}$ are the carrier frequencies and refractive indices of the pump and Stokes pulses, respectively, N is a medium density, γ is an SRS medium relaxation rate, and $r_{eff} = \frac{1}{\hbar} \sum_i \frac{d_{3i} d_{i1}}{\omega_{i3} + \omega_{i1} - \omega_p - \omega_s}$ is a Raman transition dipole matrix element [42–44]. We also assumed that the fiber is designed to suppress all but the pump and fundamental Stokes modes of molecular hydrogen [42].

Next, suppose all hydrogen molecules are in their ground states prior to interaction with the pulses and take the strong input pump pulse to be a Gaussian such that $E_p(t, 0) = |E_{p0}| e^{-t^2/2t_p^2}$, where t_p is a pump pulse duration. At the same time, we assume a weak probe Stokes pulse to be fluctuating such that at the fiber input, $E_s(t, 0) = |E_{s0}| a_s(t) e^{-t^2/2t_s^2}$, where t_s is a Stokes pulse duration and $a_s(t)$ is a dimensionless statistically stationary random amplitude. Introducing peak optical intensities of the pulses $I_{s0,p0} = \epsilon_0 n_{s,p} c |E_{s0,p0}|^2 / 2$ we scale the pulse fields to the peak pump intensity at the source, $E_p = \sqrt{2I_{p0}/\epsilon_0 c n_p} \mathcal{E}_p$ and $E_s = \sqrt{2I_{p0}/\epsilon_0 c n_p} \mathcal{E}_s$. Next, we introduce dimensionless distance and time, $Z = \zeta/l_{SRS}$ and $T = \tau/t_{SRS}$ where $l_{SRS} = (2\epsilon_0 c / N r_{eff}) \sqrt{n_p n_s / \omega_p \omega_s}$ and $t_{SRS} = 2\hbar \epsilon_0 c n_p / r_{eff} I_{p0}$ are characteristic length and time over which energy exchange between pulses and the medium unfolds. The SRS equations can then be cast into a dimensionless form as

$$\partial_Z \mathcal{E}_p = ik \sigma \mathcal{E}_s, \quad (4)$$

$$\partial_Z \mathcal{E}_s = ik^{-1} \sigma^* \mathcal{E}_p, \quad (5)$$

and

$$\partial_T \sigma = -\Gamma \sigma + i \mathcal{E}_p \mathcal{E}_s^* \quad (6)$$

Here $k = \sqrt{\omega_p n_s / \omega_s n_p}$ and $\Gamma = \gamma t_{SRS}$ is a key dimensionless parameter governing the SRS process. Further, the dimensionless initial conditions read

$$\mathcal{E}_p(T, 0) = e^{-T^2/2T_p^2}, \quad (7)$$

and

$$\mathcal{E}_s(T, 0) = \sqrt{\frac{n_p I_{s0}}{n_s I_{p0}}} a_s(T) e^{-T^2/2T_s^2} \quad (8)$$

Let us now construct an input Stokes pulse ensemble. To enhance the SRS efficiency we want to maximize the pump and Stokes pulse intensity overlap. To this end, we assume that Stokes and pump pulses have the same durations, $t_p = t_s = t_0$. We model Stokes pulses as a Gaussian random process, which is completely specified by its second-order correlation function, the mutual coherence function. The latter is assumed to be Gaussian; this is a celebrated Gaussian Schell model (GSM) of optical coherence theory [45]. With the help of Eqs. (7) and (8), the GSM mutual intensity can be expressed as

$$\Gamma(T_1, T_2, 0) \equiv \langle \mathcal{E}_s^*(T_1, 0) \mathcal{E}_s(T_2, 0) \rangle = \left(\frac{n_p \langle W_s \rangle}{n_s W_p} \right) \times \exp\left(-\frac{T_1^2 + T_2^2}{2T_0^2}\right) \exp\left[-\frac{(T_1 - T_2)^2}{2T_c^2}\right]. \quad (9)$$

Here the angle brackets denote ensemble averaging; $T_p = T_s = T_0 = t_0/t_{SRS}$ and $T_c = t_c/t_{SRS}$, where t_c is a Stokes pulse coherence time and we eliminated the pump and Stokes peak intensities in favor of the pulse energies, W_p and $\langle W_s \rangle$.

To construct the random pulse ensemble, we employ the Karhunen-Loève expansion [46]

$$\mathcal{E}_s(T, 0) = \sum_n c_n \psi_n(T), \quad (10)$$

where the random coefficients $\{c_n\}$ are orthogonal such that

$$\langle c_n^* c_m \rangle = \lambda_n \delta_{mn}, \quad (11)$$

and the coherent modes are orthonormal, implying that

$$\int_{-\infty}^{\infty} dT \psi_n^*(T) \psi_m(T) = \delta_{mn}. \quad (12)$$

The mutual coherence function is then represented as a Mercer-type series in coherent modes as [45]

$$\Gamma(T_1, T_2, 0) = \sum_n \lambda_n \psi_n^*(T_1) \psi_n(T_2). \quad (13)$$

Next, the complex random amplitudes $\{c_n\}$ can be expressed in the polar form as

$$c_n = \sqrt{i_n} e^{i\phi_n}. \quad (14)$$

We stress that Eqs. (10) through (14) describe any statistical source. Thus, we must spell out a concrete model for the random amplitudes and phases, adequately describing a given physical source. In our case, we assume random phases $\{\phi_n\}$ to be uniformly distributed in the interval $0 \leq \phi_n \leq 2\pi$, and random amplitudes $\{i_n\}$ to obey the Rayleigh distribution such that $\{i_n\}$'s are governed by the exponential distribution as

$$\mathcal{P}(i_n) = \frac{1}{\lambda_n} e^{-i_n/\lambda_n}. \quad (15)$$

Thus c_n is a complex Gaussian random variable. It follows that the incident Stokes pulse ensemble $\{\mathcal{E}_s(T, 0)\}$ is Gaussian as a sum of independent Gaussian random variables [46]. We stress that the mode power distribution of the form (15) is sufficient to guarantee Gaussian statistics of the source regardless of its temporal coherence. On the one hand, in the low-coherence limit when many coherent modes in the expansion (13) are required to faithfully reproduce the source mutual intensity, Gaussian statistics of the pulse ensemble can be ensured for any mode power distribution $P(i_n)$ by virtue of the central limit theorem [46,47]. On the other hand, however, as the source becomes sufficiently coherent such that only a few coherent modes enter Eq. (13), the central limit theorem no longer applies. Yet, the input source ensemble is Gaussian, provided it is a sum of independent modes each obeying Gaussian statistics. We note in passing that the present source ensemble is drastically different from previously considered non-Gaussian stochastic input pulses, generating random phase solitons in resonant media [37]. We also note that we focus on noise effects due to strongly fluctuating input Stokes pulses. In other words, we ignore spontaneous Raman scattering (quantum) noise which is dwarfed by thermal-like fluctuations of the incident Stokes pulses.

To complete our source modelling, we observe that the GSM eigenvalues and coherent mode profiles are given by [45]

$$\lambda_n = \sqrt{\pi}T_0 \left(\frac{n_p W_s}{n_s W_p} \right) \frac{(\alpha + \xi)\beta^n}{(\alpha + \beta + \xi)^{n+1}}, \quad (16)$$

and

$$\psi_n(T) = \left(\frac{2\xi}{\pi} \right)^{1/4} \left(\frac{1}{2^n n!} \right)^{1/2} H_n(T\sqrt{2\xi})e^{-\xi T^2}, \quad (17)$$

where $H_n(x)$ is a Hermite polynomial of the order n and we introduced the notations $\alpha = (2T_0^2)^{-1}$, $\beta = (2T_c^2)^{-1}$, and $\xi = \sqrt{\alpha^2 + 2\alpha\beta}$.

3. Numerical results

As a practical realization of the system, we consider a meter long hydrogen-filled HC PCF with typical parameters representative of the HC PCFs previously designed for SRS experiments [41, 42]. The HC PCF has a low-loss transmission window between 1030 and 1150 nm. As a result, only the pump and first Stokes modes, interacting with the $J=1$ to $J=3$ rotational transition, can co-propagate in the HC PCF. We choose a narrow linewidth laser delivering 10 ns pulses of a $20 \mu J$ energy at 1064 nm as the pump. The Stokes pulses with the mean peak power of 10 W operate at 1134 nm. Such Stokes pulses can be excited by time modulating (chopping) an output of a cw partially coherent source using, for instance, electro-optical modulators [48]. We take the relaxation time of hydrogen in the HC PCF to be $\gamma^{-1} = 5$ ns [44]; the effective Raman interaction length and time are estimated to be $l_{SRS} = 1$ mm and $t_{SRS} = 6$ ns, respectively.

We use the same numerical Monte Carlo simulation procedure as the one described in [37] in the context of random phase soliton excitation in two-level media to generate a random Stokes pulse ensemble of 2×10^4 realizations and examine its power fluctuations on pulse propagation inside the fiber. Our extensive numerical simulations indicate that power fluctuations 90 times greater than the mean power—nearly 900 W compared to the mean power of 10 W—can occur at the fiber output. We illustrate this point by exhibiting a time series of the normalized Stokes pulse powers at the fiber input and output in Fig. 1. We checked that giant power fluctuations can take place even for shorter fiber lengths. For instance, power fluctuations greater than 50 times the mean power (around 500 W) occur in 1 cm long fibers. These observations are reflected in the presence of a very long probability distribution tail in Fig. 2 where we display the normalized Stokes peak power PDF for three cases: $T_c = 10T_p$ (rather coherent input pulses), $T_c = T_p$, and $T_c = 0.1T_p$ (nearly incoherent Stokes input). All powers are normalized to the average power of

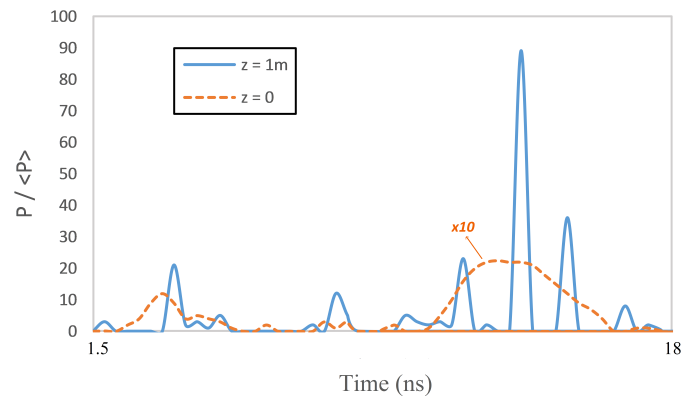


Fig. 1. Normalized (to the average power at the source) peak power fluctuations of a random Stokes pulse with $T_c = 0.1 T_0$ at the fiber output (blue) and input (orange). To facilitate the visualization, the orange curve is scaled by the factor of 10.

the input Stokes pulse ensemble. It is seen in Fig. 2 that as the Stokes source coherence time progressively increases, the probability distribution tail gradually depopulates. The exponential

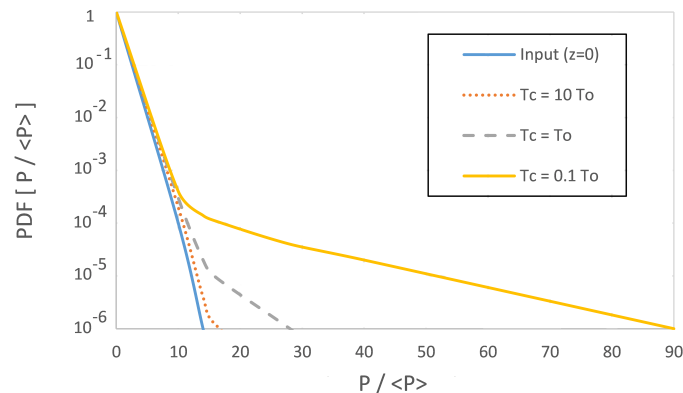


Fig. 2. Normalized Stokes pulse peak power PDF at the entrance (blue) and exit to the HC PCF. The input/output pulse power is normalized to the average power at the source. The Stokes source coherence time takes on values $T_c = 0.1 T_0$, $T_c = T_0$ and $T_c = 10T_0$.

power distribution of the input Stokes ensemble is also displayed for comparison. It can be inferred from the figure that in all three cases, the PDF, exhibited in the logarithmic scale, nearly coincides with the exponential input distribution for sufficiently low powers, but it sharply deviates from the exponential distribution in the high Stokes power limit. Thus, the PDF is strongly non-Gaussian. Moreover, the output PDF appearance—including the magnitude of its tail—can be controlled by adjusting the Stokes source coherence time.

We notice that the degree to which the peak power statistics deviates from Gaussian, sharply increases as the source coherence time shrinks. This trend is opposite to the one recently encountered for integrable turbulence governed by the nonlinear Schrödinger equation [29]. This circumstance should not be surprising as SRS is fundamentally different from the system studied in [29]. While the former unfolds as a noninstantaneous resonant light-matter interaction, described, in general, by nonintegrable nonlinear equations, the latter is essentially a weakly dispersive wave system with a weak instantaneous nonlinearity. The ORW emergence in [29] is

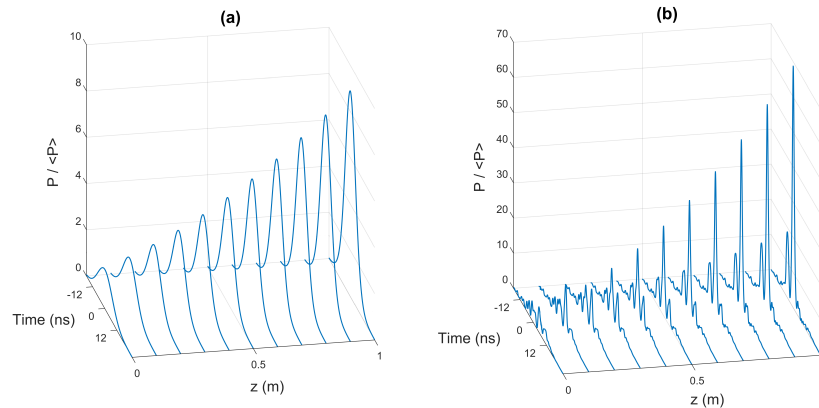


Fig. 3. Normalized (to the average power at the source) peak power fluctuations of a random Stokes pulse for (a) very coherent, $T_c = 10T_0$ and (b) nearly incoherent, $T_c = 0.1T_0$ Stokes ensemble at the source as functions of time and propagation distance.

linked by the authors to soliton and breather collisions, the frequency of which is enhanced with the source coherence time increase. The ORW generation in SRS cannot be explained by this mechanism because, even in the coherent transient limit when the input pulse duration is much shorter than the SRS medium relaxation time and the SRS equations are integrable [49], solitons are known to be transient in SRS, giving way to self-similar waves as fundamental asymptotics of the system in the long-term limit [42, 50]. Furthermore, SRS soliton lifetimes are expected to shrink as the input pulse duration becomes comparable to the SRS medium relaxation time which is the case here.

To explain the PDF tail dependence on the source coherence time in SRS, we employ the concept of statistical granularity in time. Statistical granularity implies that the SRS interaction is coherent within a time interval of t_c and Stokes pulses outside these time intervals are uncorrelated. The number of statistical granules corresponds to the effective number of coherent modes entering the Karhunen-Loève representation, Eq. (10), of the Stokes pulse ensemble. As t_c decreases, the number of uncorrelated modes (statistical granules) representing each Stokes ensemble member increases, making the Stokes source noisier. As the statistical granules are uncorrelated, they all compete for energy supply from the pump, resulting in a selective granule amplification and, eventually, leading to a giant amplitude granule formation within the Stokes pulse profile during the SRS amplification process. We stress that the long memory of the system plays an important role in facilitating selective amplification of large amplitude Stokes granules, leading to champion pulses of enormous amplitudes. This situation is vividly illustrated in Fig. 3 where we display, side by side, the Stokes ensemble member evolution as the pulse propagates along the fiber for a very coherent source, $T_c = 10T_0$, and a nearly incoherent one, $T_c = 0.1T_0$. The formation of a large amplitude statistical granule within the incoherent Stokes pulse is manifest in the figure. On the contrary, amplification is coherently distributed across the pulse profile in the coherent case, resulting in fairly uniform amplification.

The characteristic number of statistical granules present at the source is related to the source coherence time. We can estimate the number of statistical (time) granules N as an inverse of the global degree of coherence of the source. The latter is defined as $\nu = \lambda_0 / \sum_n \lambda_n$ [45]. It follows at once from Eq. (16) that for a nearly incoherent Stokes source, $T_c \ll T_p$, the number of time granules can be estimated as $N \approx \nu^{-1} \propto T_c^{-1}$. Thus, the number of statistical granules grows in inverse proportion to shrinking source coherence time, augmenting the probability of rogue-wave events, and hence the emergence of a non-Gaussian, heavy-tail statistics of the

Stokes pulse power. We note that statistical time granules are temporal analogs of spatial speckles, hypothesized to give rise to rogue waves in spatially extended systems [6, 7].

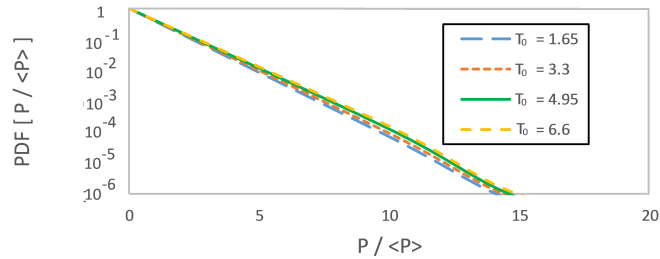


Fig. 4. Normalized (to the average power at the source) peak power PDF of the Stokes pulse ensemble at the fiber exit for highly coherent Stokes input ensemble with $T_c = 200 T_0$ for different T_0 values.

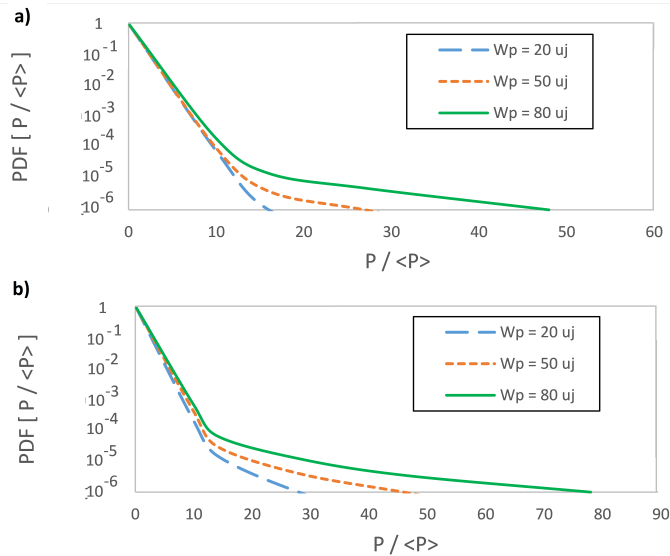


Fig. 5. Normalized (to the average power at the source) Stokes pulse peak power PDF at the HC PCF exit for different input pump pulse energies and Stokes input coherence times: a) $T_c = 10 T_0$ and b) $T_c = T_0$.

To confirm the crucial role played by the source coherence time and rule out the source nonstationarity influence, we carried out a series of simulations with highly coherent input Stokes pulse ensemble with $T_c = 200 T_0$ for different values of T_0 . The results are displayed in Fig. 4. It can readily be inferred from the figure that source nonstationarity has a negligible effect on the ensemble PDF shape at the fiber exit.

Finally, we show that a heavy-tail Stokes output statistics can be generated with not too incoherent ($T_c = T_0$) and even rather coherent ($T_c = 10 T_0$) Stokes input if we increase the pump pulse energy. As we illustrate in Fig. 5, by increasing the pump pulse energy (W_p) from $20 \mu\text{J}$ to $80 \mu\text{J}$ the statistical behaviour of the Stokes pulses begins to shift from Gaussian to highly non-Gaussian, heavy-tail statistics. This deviation is more pronounced for the less coherent case of $T_c = T_0$ in complete agreement with the just outlined qualitative picture of ORW formation in the SRS in HC PCFs.

4. Conclusion

In conclusion, we have explored a Stokes power statistics in SRS inside hydrogen filled HC PCFs. We have shown that the statistics significantly deviates from the normal distribution, exhibiting heavy tails indicative of anomalously high probabilities of extremely large amplitude output pulses. We have shown that the extreme-value output statistics strongly depends on the initial noise level of the source Stokes pulses. The latter can be conveniently controlled by adjusting the source Stokes coherence time. Thus our findings establish a clear link between optical coherence and rogue wave theories. We explain our results invoking the concepts of statistical granularity and global degree of coherence. The former emerges as a crucial driving factor behind optical rogue wave formation in transient SRS. We observe that while the medium relaxation time in solid-core fibers is so short, $\Gamma \gg 1$, that the SRS interaction is virtually instantaneous, the SRS in HC PCFs has a finite relaxation time, $\Gamma \sim 1$, and hence a non-instantaneous character. This circumstance makes the latter especially conducive to ORW formation because the noninstantaneous nonlinear light-matter interaction leads to an efficient energy redistribution to higher-energy realizations of the Stokes pulse ensemble. We anticipate our work to stimulate further theoretical and experimental investigations into rogue wave formation in nonlinear wave systems in the vicinity of optical resonances.

Funding

Natural Sciences and Engineering Research Council of Canada (NSERC) and Killam Trusts.